Effect of Postweld Heat Treatment on Weld Metal Impact Toughness of a Semi-Austenitic PH Stainless Steel

Recommendations for postweld heat treatment are made to obtain the best balance of hardness and impact values

BY N. SIVARAMAKRISHNAN, K. S. RAJA AND K. PRASAD RAO

ABSTRACT. Semi-austenitic precipitation hardened PH stainless steel plates, PH 15-7 Mo (Cu), 6.14 mm thick were autogenously welded using the electron beam welding (EBW) and plasma arc welding (PAW) processes. Impact toughness studies using Charpy V-notch samples (V-notch at the center of the weld metal) showed that EB welds had higher impact toughness than PA welds in various identical postweld heat treated (PWHT) conditions. Based on hardness and impact toughness values, the optimal postweld heat treated conditions are recommended. The effect of retained austenite, carbides and delta ferrite on impact toughness of the welds are discussed.

Introduction

Precipitation hardening (PH) stainless steels are well known for their high strength, good toughness and corrosion resistance. They are used in aerospace, marine and oil field applications as casings, welded tubes, fasteners and rods (Ref. 1). Among the three types of PH stainless steels *viz.*, martensitic, semi-austenitic and austenitic, the martensitic PH stainless steels are widely used because of their easy heat treating characteristics. So, most of the available information in open literature on PH stainless steels pertains to the martensitic type only (Refs. 2–5). Even though semi-austenitic PH stainless steels are considered to be easily formable (because of higher retained austenite) at room temperature and have easy weldability (Ref. 6), not much research has been conducted on semi-austenitic-type PH steel welds.

This steel is strengthened principally by two mechanisms: 1) transformation to the martensite; and 2) aging the martensite, which is supersaturated with copper. The steel is solution treated (ST) (homogenized) at 1050°C (1922°F) for 45 min and air cooled. For complete martensite transformation, the solution treated material is either refrigerated at 80°C (-112°F) or destabilized at around 700° to 760°C (1292°–1400°F) for about two hours and then quenched to about 5°C (40°F) in a refrigerator. During destabilization treatment, the carbon in austenite comes out and precipitates as carbides at the austenite grain boundaries. This destabilizes austenite and increases the M_s (martensite start) temperature well above room temperature. The required mechanical properties are achieved by carrying out aging treatment between 450° to 600°C (842°–1112°F). At this aging temperature, precipation of copper-rich precipitates occurs, which are coherent with the matrix and increases the hardness. At a slightly higher aging temperature of 550° to 600°C (1022°–1112°F) precipitation of fcc ε-phase occurs, which is considered an overaged condition.

As for the welding of these materials, it would be ideal to use processes with low heat input in order not to change the microstructure to a greater extent. In this context, electron beam welding may be an appropriate process. Another alternative is to use processes like plasma arc welding, which may also be considered a low heat input process, though not so low as EBW. Not much work is reported on the properties of semi-austenitic stainless steel weldments welded by these processes. In this investigation, an attempt was made to study the impact toughness behavior of a semi-austenitic PH stainless steel (SS) welded by these

KEY WORDS

Electron Beam Welds
Plasma Arc Welds
Precip. Harden. SS
Retained Austenite
Delta Ferrite
Impact Toughness
PWHT
Hardness
Grain Size
Cooling Rate

N. SIVARAMAKRISHNAN, K. S. RAJA and K. PRASAD RAO are with the Department of Metallurgical Engineering, Indian Institute of Technology, Madras, India.

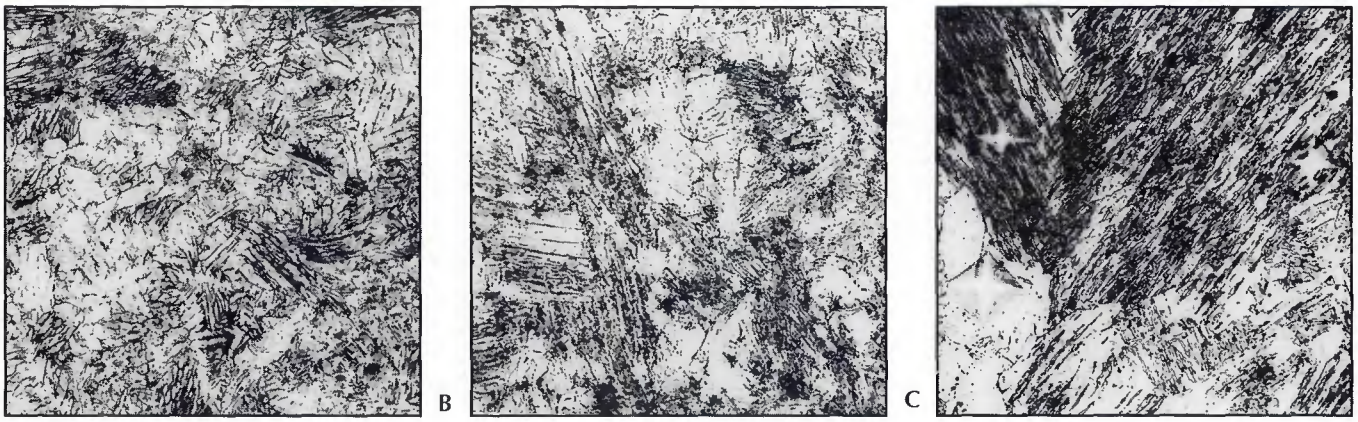

Fig. 1 — Optical and x-ray diffraction examination of EB and PA welds. A — Microstructure of as-welded EB specimen, 200X; B— microstructure of as-welded PA specimen, 200X; and C — microstructure of as-welded PA specimen. White etched region is austenite. Martensite is etched dark. Large and small hardness indentations on the respective phases confirm this.

processes (thereby, two different heat inputs): electron beam welding (EBW) and plasma arc welding (PAW).

Experimental

Steel plates, PH 15-7 Mo (Cu), 6.14 mm (0.24 in.) thick were taken in solution treated (mill annealed) condition and cut in the L-S direction to strips of 300 x 55 x 6.14 mm (11.8 x 2.2 x 0.24 in.). The chemical composition of the material is given in Table 1. The surfaces of the strips were ground using abrasive belt of 180 grit, emery papers of grades 1/0, 2/0, 3/0, 4/0, polishing abrasive of alumina powder and diamond paste to remove the top oxide layer, and then cleaned with soap water followed by acetone.

Autogenous bead-on-plate electron beam welding was carried out along the center of the strips to get a through thickness penetration. A 12-kW capacity, 150-kV Hawker Siddeley EBW machine was used. The welding details are given in Table 2. The second lot of strips were welded autogenously by the plasma arc welding process. In order to get through thickness penetration, opposing autogenous PAW beads were put on both sides of the strips. The interpass temperature was maintained at room temperature. The welding details of PAW are given in Table 3. Addition of filler metal was avoided so that the same chemical composition in both types of welds could be achieved.

Charpy V-notch (V-notch at the center of the weld) samples were machined out of the welded plates and different lots of samples were subjected to three different postweld heat treatment (PWHT) cycles as follows:

1) welded and aged.

2) welded, destabilized and aged.

3) welded, solution treated, destabilized and aged.

Aging was carried out at three different

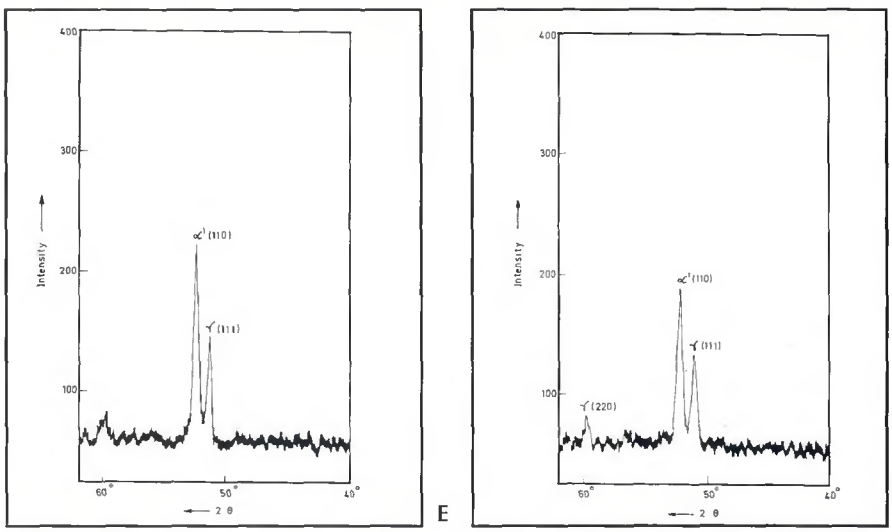

D — XRD profile of EB weld (welded then aged at 450°C/3 h); E — XRD profile of PA weld (welded then aged at 450°C/3 h).

Table 1 — Chemical Composition

Element	%	Element	%	Element	%
C	0.054	S	0.010	Mo	1.368
Si	0.455	Co	0.058	Cu	2.890
Mn	0.822	Cr	14.530	Ti	0.305
P	0.026	Ni	6.920	Fe	Balance

Table 2 — Welding Parameters of EBW

Beam current	— 60 mA
Accelerating voltage	— 100 kV
Speed of welding	— 130 cm/min
Work-to-gun distance	— 43 cm
Gun vacuum	— 10^{-5} torr
Chamber vacuum	— 10^{-4} torr
Type of filament	— Ribbon (Strip) type

Table 3 — Welding Parameters of PAW

Current	— 150 A
Voltage	— 20 V
Welding speed	— 30 cm/min
Plasma gas and shielding gas	— Argon
Plasma gas flow rate	— 4.5 L/min
Shielding gas flow rate	— 9.0 L/min

A

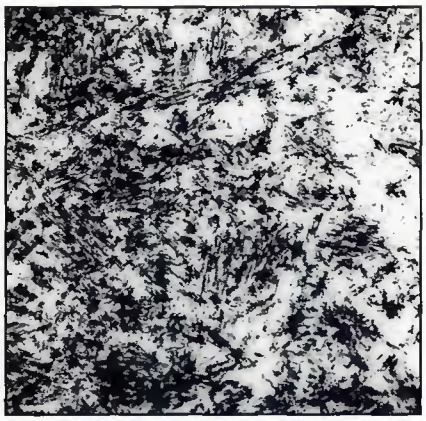

B

Fig. 2 — Optical examination of destabilized welds and XRD profiles of destabilized and aged welds. A — Microstructure of EB weld specimen, 200X (welded, destabilized); B — microstructure of PA weld specimen, 200X (welded, destabilized);

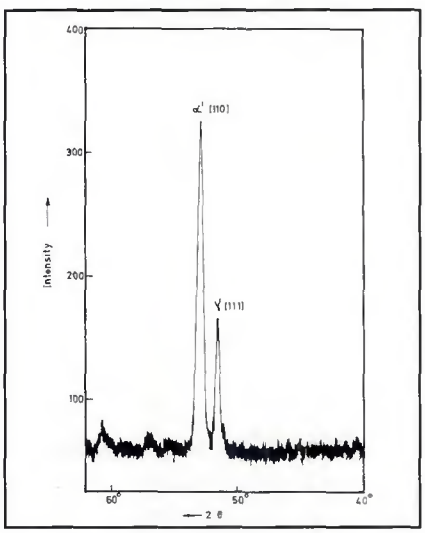

C

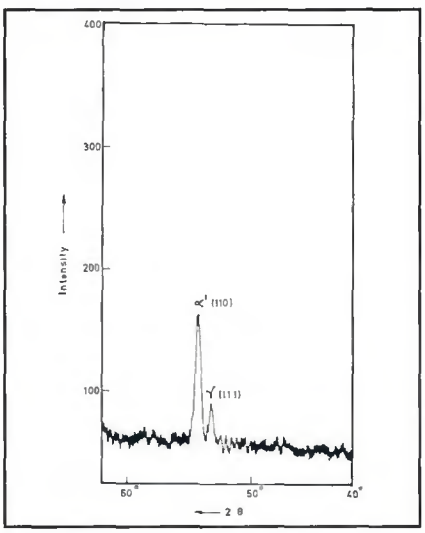

D

C — XRD profile of PH 15-7 Mo (Cu) EB weld (as-welded); D — XRD profile of EB weld (destabilized, aged at 450°C/3 h);

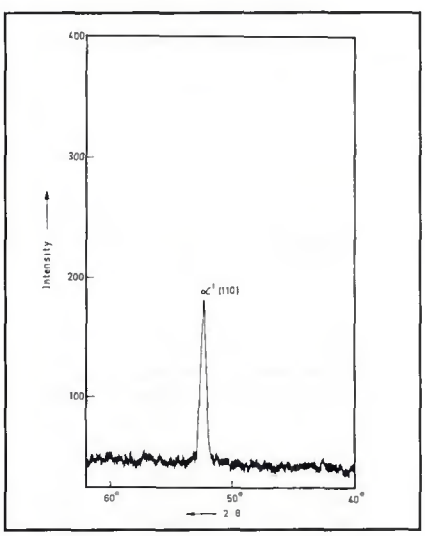

E

E — XRD profile of PA weld (destabilized, aged at 450°C/3 h).

temperatures and times: 1) 450°C for 3 h; 2) 480°C for 4 h; and 3) 550°C for 1 h.

The destabilization treatment was given at 760°C for 2 h; air cooled and quenched to about 5°C.

The solution treatment was given at 1050°C for about 45 min and air cooled.

After PWHT, the Charpy V-notch samples were tested at room temperature for their impact toughness. Five samples were tested at each condition, and the average values are reported. Fracture surfaces were observed with a scanning electron microscope (SEM), and energy dispersive x-ray (EDX) patterns were taken at selected regions. The face of the weld specimens were polished to 1 μm finish and etched with Fry's reagent (which is prepared by dissolving 5 g of cupric chloride in 40 mL concentrated HCl + 30 mL methyl alcohol + 30 mL water). The etching was carried out by swabbing with the solution for 30 s to reveal both martensite and δ-ferrite structures. Then light optical microstructure and Vickers hardness studies were carried out. X-ray diffraction (XRD) analysis was carried out using CoK_α radiation on EB and PW welds to determine the relative proportions of austenite and martensite phases.

Results

Microstructure

Figure 1A and B show the optical microstructure of the EB and PA welds in the as-welded condition. The EB weld contains relatively smaller grains when compared to that of the PA weld. Higher cooling involved with the EBW process can be attributed to the reason for smaller grains. The microstructure of the as-welded metal consists of a delta ferrite network in a martensite and austenite matrix. Since the as-welded condition represents a solution treated condition, a relatively large amount of austenite is expected to be retained in the weld metal as the M_f temperature falls well below the room temperature and no subzero treatment is given to the weld metal. Through a microhardness survey, it was found that the white regions distributed in the microstructure could be austenite, as the hardness was very low (240 VHN) when compared to the black lath type structure (340 VHN), as shown in Fig. 1C. It can be observed from microstructures that EB weld metal contains a larger amount of austenite than the PA weld metal. It was found that by carrying out the aging treatment of the as-welded samples on both welding processes did not alter the optical microstructures. This can be due to two reasons: 1) aging temperatures are far below the transformation temperature of the material; and 2) the precipitation of copper-rich precipitates is submicroscopic in nature and cannot be seen in optical microstructure. Moreover, the presence of a large amount of austenite will not aid precipitation since austenite can dissolve more copper and carbon.

Figure 2A shows the microstructure of EB weld metal, which was destabilized. When comparing the microstructures of as-welded and destabilized weld metal, it can be observed that the latter contains a higher amount of martensite (dark-etched portions). But the dendritic type of structure is clearly visible, which indicates that the recrystallization and homogenization processes are not complete. Figure 2B shows the microstructure of the destabilized PA weld metal. In the case of PA weld metal, the dendritic solidification pattern is not clearly visible. But when compared to the PA as-welded microstructure, the destabilized microstructure was found to be altered. This could be due to the dissolution of some amount of delta ferrite

in the austenite and the transformation of austenite to martensite by destabilization treatment. XRD analysis indicated that after destabilization followed by aging, the integrated intensity of the austenite peak was lower (Fig. 2D) when compared to that of the as-welded (Fig. 2C) and as-welded plus aged condition (Fig. 1D) for the EB weld. In the case of the PA weld, there was no distinguishable austenite peak after destabilization treatment (Fig. 2E) when compared to that of as-welded plus aged condition — Fig. 1E.

Figure 3A shows the microstructure of the EB weld with a solution treated plus destabilized condition. The dendritic weld structure, which was observed in the as-welded (Fig. 1A) and destabilized condition (Fig. 2A), is not observed in the solution treated plus destabilized PWHT condition. The solution treated plus destabilized PA weld metal also showed the same kind of microstructure (Fig. 3B) as the EB weld metal, but the grain size was different. It was found that the EB weld metal had higher retained austenite than the PA weld metal. X-ray diffraction analysis also supported this. Figure 3C and 3D show the XRD analysis of the solution treated plus destabilized plus aged at 450°C for 3 h EB and PA weld metals, respectively. By comparing the integrated intensities of martensite and austenite peaks, it can be observed that the EB weld had higher austenite content than the PA weld metal of identical PWHT.

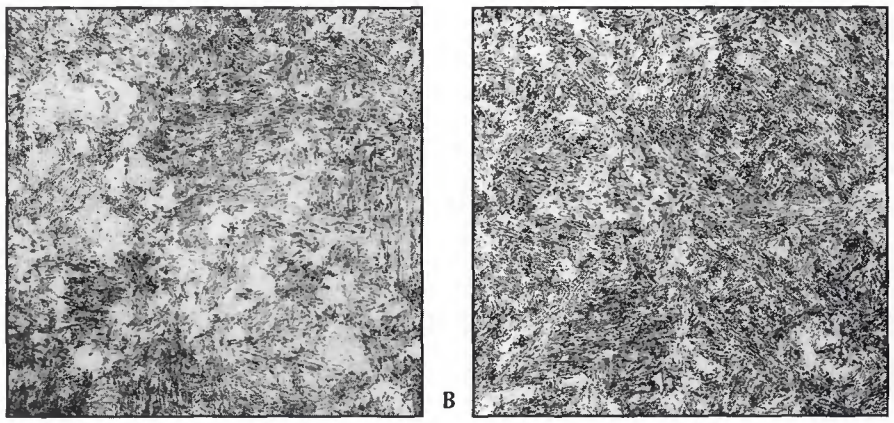

Fig. 3 — Optical examination and XRD profiles of solution treated, destabilized welds. A — Microstructure of EB weld specimen, 500X (welded, solution treated, destabilized); B — microstructure of PA weld specimen, 500X (welded, solution treated, destabilized);

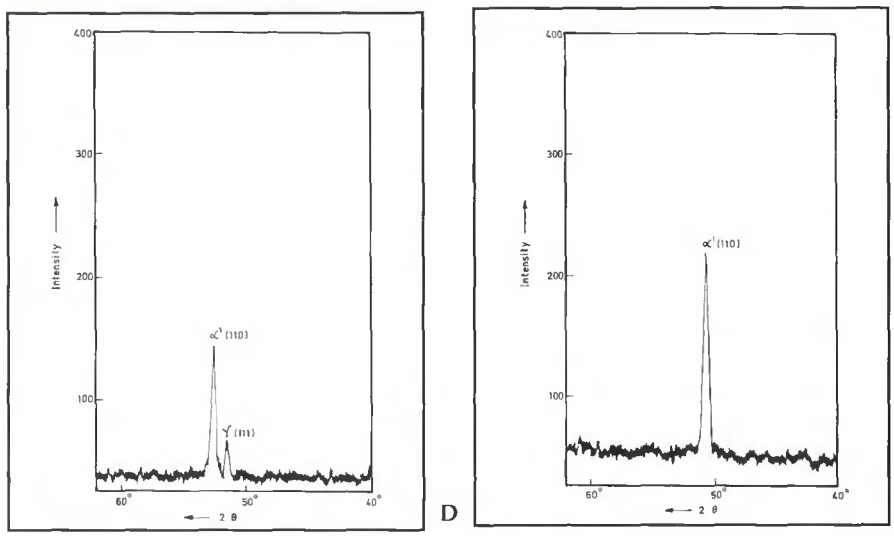

C — XRD profile of EB weld (welded, solution treated, destabilized, aged 450°C/3 h); D — XRD profile of PA weld (welded, solution treated, destabilized, aged at 450°C/3 h).

Hardness

Figure 4A –C shows the hardness values of EB and PA welds with various PWHT. As-welded samples of EB and PA welds had very low hardness, when compared to other PWHT conditions. This lower hardness is attributed to the presence of retained austenite and as transformed martensite, which is unaged. Aging the weld metal without the prior destabilization treatment did not increase the hardness to any appreciable level — Fig. 4A. This is due to the presence of untransformed austenite, which dissolves more copper. It can be observed that the as-welded EB weld metal had higher hardness than its PA weld counterpart. This is attributed to the smaller grain size of the EB weld.

Destabilization followed by aging increased the hardness of both EB and PA weld metals owing to the fact that destabilization caused dissolution of ferrite and strengthened the matrix by precipitating the coherent copper-rich precipitates. When compared, the PA welds showed higher hardness at 450° and 480°C aging treatments than that of the EB weld counterparts. The amount of retained austenite is more in EB welds than in PA welds — Fig. 2A. The possible segregation of alloying elements, such as copper, that leads to nonuniform distribution of precipitates in the matrix of the EB weld may be due to the dendritic microstructure, even though by convention there is more segregation in the PAW than the EBW process.

When solution treated, the weld metals of the PA and EB welding processes were found to be homogenized. This led to uniform increase in hardness throughout the weld metal when the same was destabilized and aged. From the hardness results, it was observed that aging at 450°C for 3 h yielded peak hardness values and aging at 550°C caused an overaged condition, whereas aging at 480°C for 4 h treatment fell in between 450° and 550°C treatments in terms of hardness and toughness, which will be discussed subsequently.

Impact Toughness

Figure 5A shows the Charpy V-notch toughness values of EB and PA welds in as-welded and aged conditions. It can be observed that the EB welds showed higher impact energy values than the PA welds. Aging at 450°C for 3 h was found to have lower impact energy than other aging treatments, even though the weld metals were not destabilized. This implies localized precipitation strengthening of the weld metal at the martensite. Aging at 550°C improved the toughness values of the as-welded condition in both the welding processes. This could be due to the reversion of austenite at this aging temperature. Austenite was found to form at martensite lath boundaries in the case of 17-4 PH stainless steel that was aged at 550°C (Ref. 2). The same kind of reversion could have taken place here also and optical metallography supports this.

Figure 5B and C show the impact toughness values of EB and PA welds with destabilized, aged and solution treated, destabilized, aged treatments,

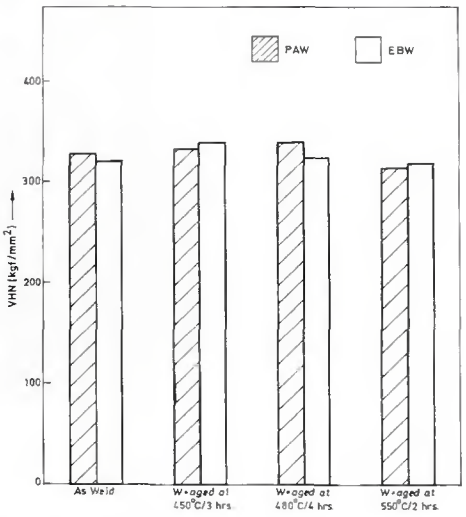

Fig. 4 — Macrohardness measurements of PA and EB welds. A — Macrohardness of PA and EB aged welds;

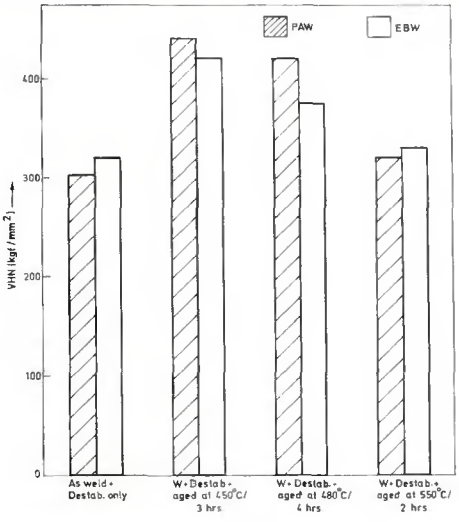

B — macrohardness of PA and EB destabilized, aged welds;

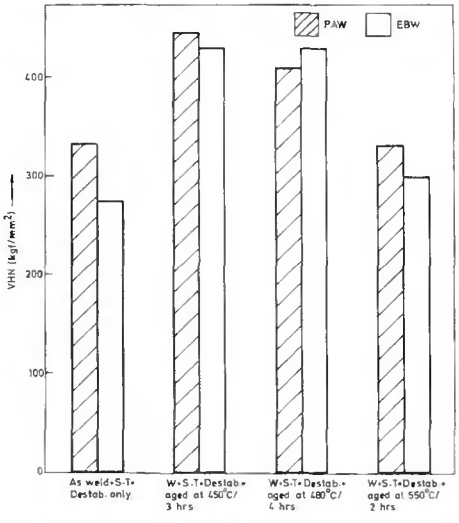

C — macrohardness of PA and EB solution treated, destabilized, aged welds.

respectively. The EB welds were found to have higher impact toughness values than PA welds in all PWHT conditions. In peak aging condition (450°C, 3 h), the welds showed lower impact energy, and the overaged condition (550°C, 1 h) had higher toughness for both the welding processes, in all the three PWHT cycles.

When comparing the three different PWHT cycles, it can be found that the as-welded and aged PWHT cycles showed maximum resistance to fracture due to impact loading. This is true for both the EBW and PAW processes. Welds that were destabilized and then aged were found to have lower impact energy values when compared to that of aged PWHT samples with identical aging treatments. Interestingly, when the welds were solution treated, destabilized and aged, the impact toughness improved a little, but they were inferior to the as-welded, aged samples.

Fractography and EDX

Figure 6A shows the fracture surface of EB weld metal in the as-welded condition. The fracture was found to be predominantly ductile, as suggested by the presence of dimples. But at some regions, the ductile-to-quasicleavage transition could be observed. The transition could be due to the presence of martensite. Energy dispersive x-ray analysis (EDX) suggested that the inclusion could be a compound of sulfide and silicate since sulfur and silicon peaks were obseved — Fig. 6B.

Figure 7A is a typical fractograph of a PA weld in the as-welded condition. Even though the PA weld had better impact toughness in the as-welded condition, some regions showed quasicleavage type fracture as shown in Fig. 7A. The ductile to quasicleavage transition was found to occur with the presence of undissolved carbides. EDX analysis showed (Fig. 7B) the presence of TiC, as titanium peak was predominant in that area. Since TiC is expected to precipitate inside the grain, no intergranular cracking was observed.

Figure 8A shows the fractograph of PA weld, which was destabilized and aged at 450°C for 3 h. Transgranular failure with dimples and secondary cracks were observed. Figure 8B shows the fracture surface of a destabilized, overaged PA weld sample. The EDX pattern in Fig. 8C indicates the presence of sulfide inclusions.

Figure 9A is the typical fractograph of an EB weld that was solution treated, destabilized and aged at 450°C for 3 h. It can be observed that secondary cracking occurred at the austenite grain boundaries, but the fracture occurred by tearing of individual martensite laths, as ob-

served from the SEM picture. Dimples are almost absent and the fracture surface is almost flat in this case. This sample showed peak hardness values and lower impact toughness when compared to other aging conditions.

Discussion

The advantage of electron beam welding of 17-4 PH stainless steel was reported by Chen and Yeh (Ref. 5). The EBW process is considered superior to others because of its advantages like a deep and narrow weld zone, reduced heat-affected zone, ability to control gas content and high reliability (Ref. 7). Because of its low heat input and high energy intensity, the cooling rate of the weldment was very high. This higher cooling rate was found to impart smaller grain size in weld metal and phase transformations in certain alloys. But Gooch (Ref. 6) reported that the EBW process caused higher retained austenite content in semi-austenitic PH stainless steel weld metal than the GTAW process.

Nageswara Rao, *et al.* (Ref. 8), has reported that higher retained austenite content and smaller prior austenite grain size improved the impact toughness of 17-4 PH wrought materials. The advantage of retained austenite on impact toughness properties has already been documented by other work (Refs. 5, 6).

From XRD analysis and light optical metallography results, the higher impact toughness of the EB welds can be attributed to the presence of higher retained austenite and smaller grain size when compared to the PA welds.

From Fig. 7B it can be seen that in the as-welded condition, the PA weld contained undissolved titanium carbide. But in the case of the EB welds, due to high heat input, all the carbides were dissolved. This stabilizes the austenite more strongly. Apart from retained austenite and grain size, the other factors that contribute to the impact toughness properties are inclusion contents, presence of carbides, delta ferrite, intertitials like hydrogen, etc., and the size and structure of copper-rich precipitates.

It is a well-established fact that inclusions like oxides, silicates and sulfides, act as crack initiation sites or change the morphology of fracture from ductile to brittle (Ref. 8). Ramsay, *et al.* (Ref. 9), investigated the effect of nonmetallic inclusions, size and population on the microstructure of HSLA steel weld metal. He found that higher inclusion content refined the martensite packet size and refined the austenite grain size. Lowering the heat input increased the advantageous effect of inclusions. In this present investigation, no efforts were made to study the effect of inclusion content on

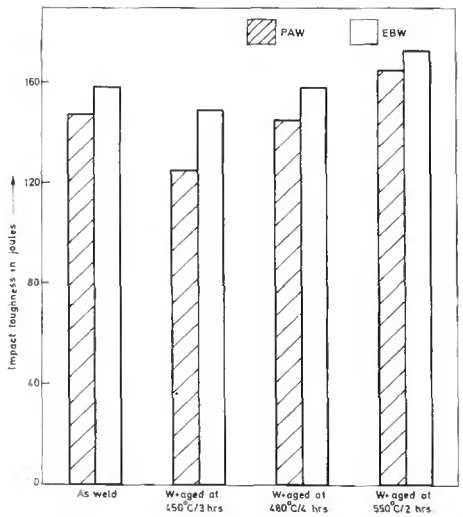

Fig. 5 — Impact toughness testing of PA and EB welds. A — Toughness of PA and EB aged welds;

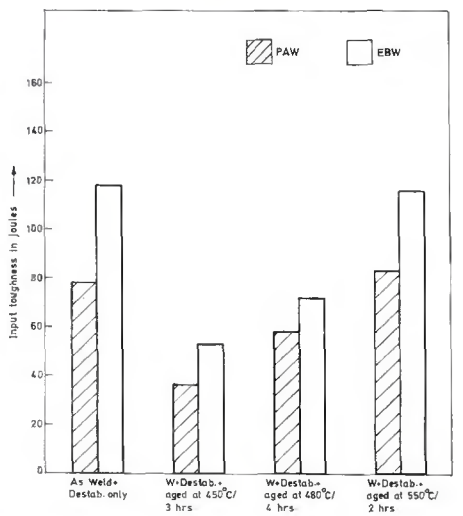

B — toughness of PA and EB destabilized, aged welds;

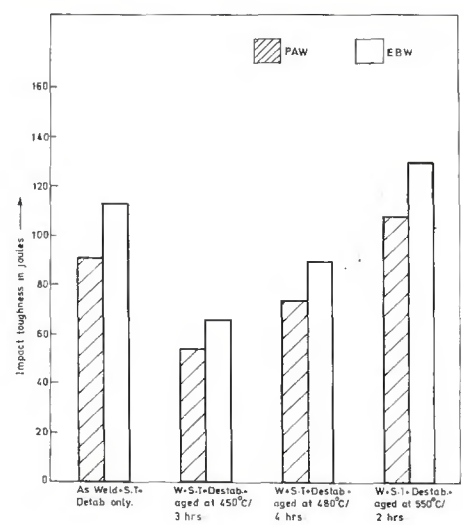

C — toughness of solution treated, destabilized, aged welds.

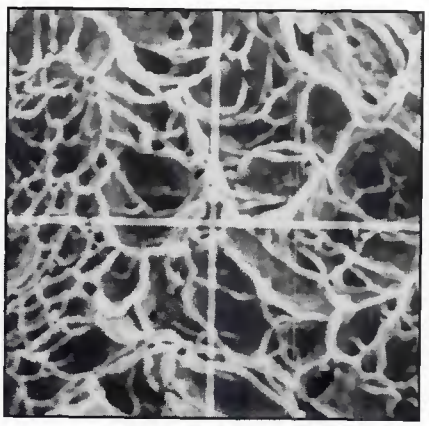

Fig. 6 — A — SEM fractograph of EB weld, 2500X (as-welded);

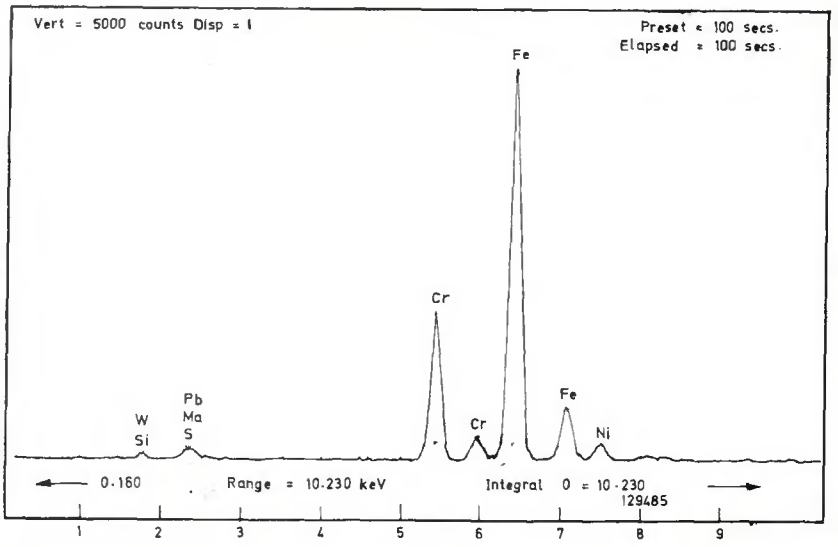

B — EDX spectra of EB weld metal.

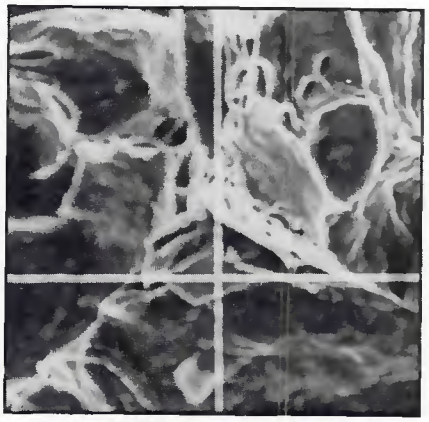

Fig. 7 — A — SEM fractograph of PA weld, 2500X (as-welded);

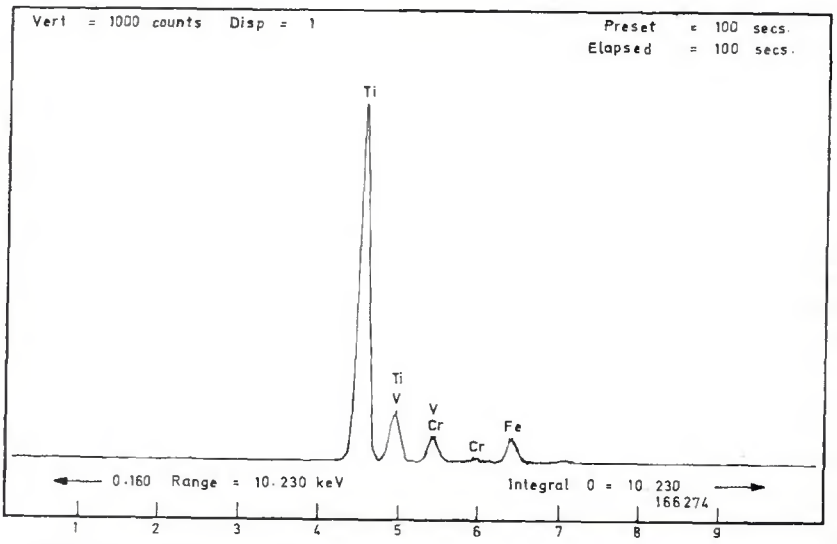

B — EDX spectra of PA weld metal.

impact toughness. But in general, it was found that the presence of inclusion at crack propagation planes changed the crack morphology from ductile (dimples) to a brittle (quasicleavage) mode. Precipitation of carbides along the grain boundary or twin boundary is also reported to decrease the impact toughness values and ductility in the case of martensitic stainless steels (Ref. 10). A high density of relatively coarse carbides was reported to favor cleavage fracture in 17-4 PH steel (Ref. 11).

Delta ferrite is a relatively soft and heat treatable phase present in the PH stainless steel weld metal and wrought metal. In the as-welded condition, it is present as a network solidified at the interdendrites of austenite — Fig. 10A. High-temperature treatments, such as destabilization or solution treatment, change the delta ferrite structure. Solution treatment is reported to decrease the delta ferrite content both in the weld metal and base metal (Ref. 2). During destabilizing treatment, delta ferrite-austenite/martensite interfaces act as potential nuclei for carbide precipitation. The higher delta ferrite content increases the carbide precipitation. It is a well-established fact that these carbides are potential sites for initiation of cleavage cracks. Slow cooling in the range of 1000° to 600°C (1832°–1112°F) could result in heavy carbide precipitation at delta ferrite-austenite interfaces (Ref. 8). So, by carefully controlling the process, this carbide precipitation could be checked, and better toughness properties can be attained. It can be observed that the impact toughness is influenced by welding heat input. Moreover, it can be observed that lower heat input (higher cooling rate) is advantageous. Higher cooling rate causes smaller austenite grain size. Moreover, a higher cooling rate causes a smaller size of martensite packets. The precipitation of carbides along the delta ferrite-austenite interface is found to be affected by higher cooling rate. So, the higher impact toughness values observed in the case of EB welds in all PWHT conditions can be directly related to the higher cooling rate of the welds. But it should be noted that the martensitic transformation temperature is not affected by the cooling rates (Ref. 10).

In order to make the martensitic transformation complete and to attain the required strength and toughness properties, postweld heat treatment is given. It could be observed that if the service requirement is more concerned about the toughness at the joints, the as-welded condition itself will yield good results, even though the base metal is in an aged condition, but the hardness of the weld metal would be very low when compared to the base metal. If the weldment is given an overaging treatment (550°C, 1 h), then the hardness would be the same throughout the weldment and the toughness would be very high. If the service requirement is concerned with strength, the weld metal should be destabilized. Destabilization causes carbon to come out and precipitate as carbide along prior austenite grain boundaries. Complete martensite transformation is found to occur by this treatment. Further aging at 450° or 480°C increases the strength but reduces the toughness. EB welds were found to possess higher toughness than PA welds. This is due to the smaller grains of the EB welds. Moreover, the amount of retained austenite was found to be more in the EB welds, which would hinder the crack propagation and increase the energy absorbed during fracture. Aging at 550°C also increases the austenite content by reverting the martensite to austenite (Ref. 2). Since the destabilization treatment was found not to be effective in homogenizing the composition and recrystallization, the dendritic microstructure was prevalent. But such microstructure was not observed in the case of PA welds.

The PA welding involved two passes back to back. During second pass welding, the weld by the first pass would have been postweld heat treated due to the heat of the second pass. Some region of the first pass weld would have experienced a temperature range of 700° to 760°C (1292°–1400°F) and carbides would have precipitated, which would reduce the toughness in the as-welded condition itself. Further destabilization would still increase the amount of carbide precipitation and decrease the impact resistance further when compared to the single pass EB welds. In this investigation, the effect of two passes in PA welds is not studied.

Solution treatment was found to be effective in homogenizing the composition and bringing the equiaxed microstructure to the weld metal. But, even after solution treatment, destabilization, the EB weld contained more retained austenite than the identical PWHT PA weld. The reason can be attributed to the fully austenite structure at the solutionizing temperature. Segregation of austenite stabilizing elements also could be high

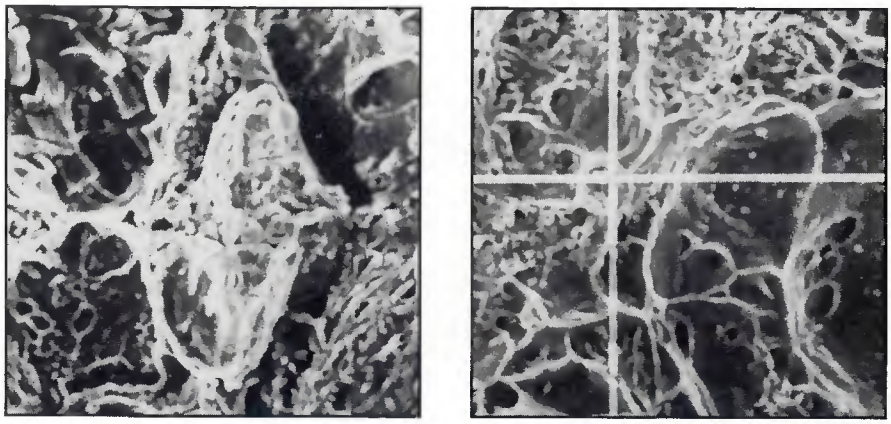

Fig. 8 — A — SEM fractograph of PA weld, 2500X (destabilized, aged at 450°C/3 h); B — SEM fractograph of PA weld 2500X (destabilized, aged at 550°C/1 h);

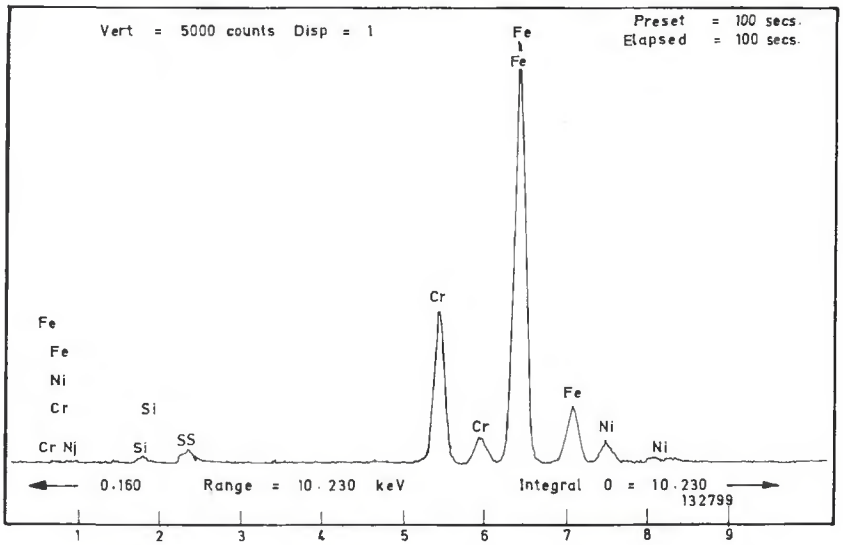

C — EDX spectra of PA weld metal in the destabilized, aged condition.

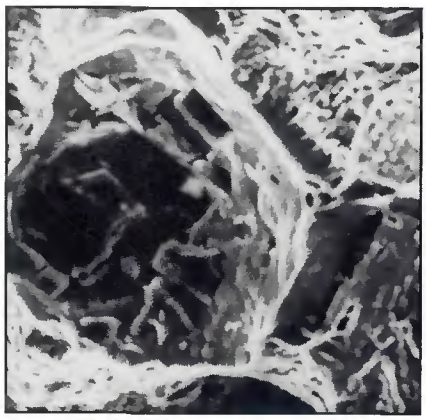

Fig. 9 — SEM fractograph of EB weld (solution treated, destabilized, aged at 450°C/3 h).

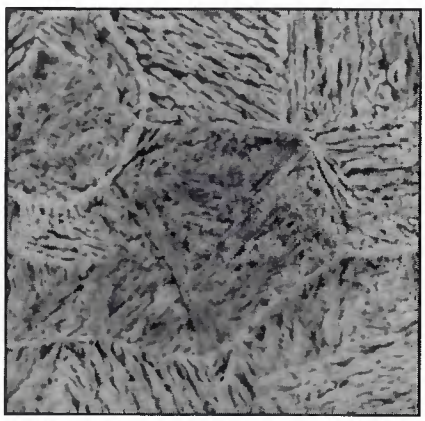

Fig.10 — SEM micrograph of as-welded PA weld metal (delta ferrite network clearly seen).

with the EBW process. This may imply that the EB weld requires long heat treatment cycles for homogenization or subzero temperature treatment for complete martensite transformation.

Conclusions

1. The samples welded by the electron beam (EB) welding process showed higher impact toughness values in all the PWHT conditions than the plasma arc (PA) welded counterparts.

2. Due to a higher cooling rate, the EB welds had smaller grain size than PA welds.

3. Higher retained austenite content increased the energy absorbed during fracture.

4. As-welded and aged EB and PA welds had higher impact toughness than other PWHT treated samples, but the hardness was low.

5. Solution treated, destabilized welds had higher hardness and moderate toughness.

References

1. Kovesi, P., and Allen, G. B. 1970. *Martensite, Fundamentals and Technology.* Edited by E. R. Petty, Longman Publications, U.K., 0.171.

2. Viswanathan, U. K., Banerjee, S., and Krishnan, R. 1988. Effect of aging on the microstructure of 17-4 PH stainless steel. *Mater. Sci. and Eng.* A104; pp. 181–189.

3. Baduri, A. K., and Venkadesan, S. 1989. Microstructure of the heat-affected zone in 17-4 PH stainless steel. *Steel Research,* Vol. 60, No.11, 509–513.

4. Islam, M. U., Campbell, G., and HSu, R. 1989. Fatigue and tensile properties of EB welded 17-4 PH steel. *Welding Journal* 68(9): 45–50.

5. Chen, C., and Yeh, J. S., Electron beam and plasma arc welding of 17-4 PH stainless steel. *Proceedings on Power Beam Processes,* San Diego, Calif., ASM International, Materials Park, Ohio, pp. 45–53.

6. Gooch, T. G. 1974. Stress corrosion cracking of welded joints in high strength steels. *Welding Journal* 53(7): 287-s to 298-s.

7. Russel, J. D. 1981. Development of heavy section EB welding, *Metal Construction* 13(10): 49–52.

8. Nageswara Rao, M., Lerch, B., and Gerold, V. 1985. Factors influencing the toughness of a 17-4 stainless steel, 76(5): 330–337.

9. Ramsay, C. W., Matlock, D. K., and Olson, D. L. 1990. The influence of inclusions on the microstructre and properties of a higher strength steel weld metal. *Proceedings of Recent Trends in Welding Science and Technology,* ASM International, Materials Park, Ohio, pp. 763–768.

10. Pickering, F. B. 1976. Physical metallurgy of stainless steel developments. *Int. Metals Reviews,* Vol.21, pp. 227–268.

11. London, P. R., Caliguri, R. D., and Duletsky, P. S. 1983. The influence of $M_{23}(CN)_6$ compound on the mechanical properties of Type 422 stainless steel. *Met. Trans. A,* Vol. 14A, pp. 1395–1408.